PCCP

Journal Name

ARTICLE

Discriminative modulation of the highest occupied molecular orbital energies of graphene and carbon nanotubes induced by charging

Hongping Yang [a], Chi-yung Yam [b], Aihua Zhang [c], Zhiping Xu [d,e], Jun Luo *[a,d] and Jing Zhu *[a,d]

The highest occupied molecular orbital (HOMO) energies of carbon nanotubes (CNTs) and graphene are crucial in fundamental and applied researches of the carbon nanomaterials, and so their modulations are desired. Our first-principles calculations reveal that the HOMO energies of CNTs and graphene can both be raised by negatively charging, and that the rising rate of the HOMO energy of a CNT is much greater and faster than that of graphene with the same C atom amount. This discriminative modulation holds regardless of the C atom amount and the CNT types, and so is universal. This work provides a new opportunity to develop all-carbon devices with CNTs and graphene as different functional elements.

1 Introduction

Carbon nanotubes (CNTs) and graphene have been extensively investigated experimentally[1-24] and theoretically,[3,21-38] due to their striking properties of electronics,[2,24] optoelectronics,[4] photonics,[5] photovoltaics,[6] energy conversion,[7] mechanics,[8,9] field emission[10,11] and secondary electron emission.[12,13] These properties originate from their unique crystal and electronic structures,[18,19,25,26,37] where the highest occupied molecular orbital (HOMO) energy plays a key role. It determines the position of the HOMO level and thus the performances of single-electron devices,[14] field emission devices[10,15] and secondary electron emitters[12,16] based on CNTs and graphene. Hence, it is significant to develop approaches to modulate the HOMO energies of CNTs and graphene and to investigate their mechanisms.

Applying an external electric field and charging have been widely used to adjust the HOMO energies,[10,14,15,28,29] of which charging easily takes place on CNTs and graphene. For example, when working as Coulomb islands in single-electron devices or emitters in field emission devices, CNTs or graphene often carry extra charges.[10,14,15] More commonly, scanning electron microscope (SEM) is one of the instruments most widely used to characterize CNTs and graphene, where the carbon nanomaterials irradiated by the electron beam of SEM are charged negatively before their secondary electron emission.[12,13,28,29] This charging has been recognized to raise the HOMO energy of single-walled CNTs by first-principles calculations,[28,29] and so the electrons at the HOMO level can be easily kicked out by the electron beam, enabling the ultrahigh secondary electron emission of the CNTs, whose secondary electron yields are 12~123 under the irradiation of the electron

beam with the accelerating voltage of 1 kV.[12] These values are comparable to that of diamond.[39] In contrast, the secondary electron yields of monolayer graphene are only 0.08~0.14 under the same condition.[13] The different experimental results imply that the modulation of the charging on the HOMO energy of graphene may be different from the one on the CNTs, which provides a new opportunity to construct all-carbon devices with CNTs and graphene as different functional elements. For example, vacuum electronic devices have been widely employed in communication, radar, space probe, guidance and heating, and their cathodes and anodes/collectors are necessarily made of materials with the properties of high and low secondary electron emission, respectively.[12,13,16] Therefore, CNTs and graphene can be used to make their cathodes and anodes/collectors, respectively. However, neither the modulation of charging on the HOMO energy of graphene nor the comparison between the modulations on graphene and CNTs has been investigated theoretically or quantitatively so far.

In this contribution, we employ the first-principles calculations with the hybrid density functional theory (DFT) method in the Gaussian09 program package on a single-walled CNT with the chirality of (3,5) and a graphene sheet (GS) whose structure is obtained by unzipping the (3,5) CNT. The calculation results indicate that the HOMO energies of both of the CNT and the GS rise with the increase of the extra electrons carried by them. More significantly, the HOMO energy of the charged CNT is generally higher than that of the charged GS, and the rising rate of the former is larger than that of the latter. The discriminative modulations persist when the C atom amount of the CNT/GS is increased from 60 to 100. Further, the discriminative modulations also work on the (5,5), (10,0)

and (6,0) CNTs and their unzipped GSs with different C atom amounts from 60 to 100. Because the above CNTs include all kinds of single-walled ones, such as chiral, armchair, zigzag, metallic and semiconducting, our finding of the discriminative modulations is universal and so is the origin and mechanism of the experimental difference of the secondary electron emissions of single-walled CNTs and monolayer graphene.

2 Simulation models and calculation method

Fig. 1(a) shows the model of a chiral (3,5) CNT containing 80 C atoms and terminated by H atoms. Its GS counterpart was constructed by unzipping its model along the tube axis, as displayed in Fig. 1(b). The GS model also contains 80 C atoms, and its edges are also terminated by H atoms, in order to warrant the validity of the comparison between the CNT and the GS. Fig. 1(c-h) depicts the models of the (5,5), (10,0) and (6,0) CNTs and their GS counterparts constructed by the same method as the above, of which the (5,5), (10,0) and (6,0) CNTs are typically metallic armchair, semiconducting zigzag and metallic zigzag, respectively.[25,29] The models of the above CNTs and GSs with nearly 60, 70, 90 and 100 C atoms have also been constructed by the same method. All of the models are neutral and do not carry any extra electrons. Their electronic structures and those of their negatively-charged cases were all calculated by the hybrid DFT method, where the amount of the extra electrons carried by the models were set from zero to eight with the increment of one. Becke's three-parameter exchange functional[40] with the Lee-Yang-Parr fit for the correlation functional[41] and the standard 6-31G(d) basis set[42,43] were applied using the Gaussian09 program package.[44] We firstly optimized the structures of the models carrying different amounts of extra electrons at the B3LYP/6-31G(d) level with different spin multiplicities, and then selected the ones with the lowest total energies as the ground state.
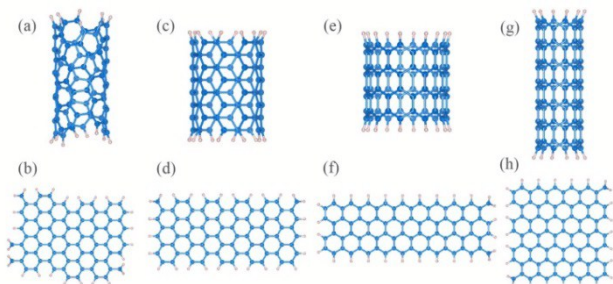
Fig. 1 Models of CNTs and GSs containing nearly 80 C atoms. (a, b) (3,5) chiral CNT and its unzipped GS, both of which contain 80 C atoms. (c, d) (5,5) armchair CNT and its unzipped GS (80 C atoms). (e, f) (10,0) semiconducting zigzag CNT and its unzipped GS (80 C atoms). (g, h) (6,0) metallic zigzag CNT and its unzipped GS (84 C atoms), where the reason to use not 80 but 84 C atoms is to keep the edges of the (6,0) models as smooth as the others. All of the models are terminated by H atoms to avoid dangling bonds.

Figs 2 and 3 give the optimized ground-state structures of the models with zero and one extra electrons, respectively, all of which only have slight differences from those in Fig. 1 at their edges and are similar to those with extra electrons of 2~8. This is rational, because the amounts of extra electrons are very small relative to the total atom amount of each model.[29] All of the optimized structures were used to calculate the electronic structures of the CNTs and GSs, which gave the HOMO

energies. In order to evaluate the accuracy of our calculations, we firstly calculated and found the average work function of the (5,5) CNT to be 4.26 eV. This value is in an excellent agreement with the one (4.68 eV) reported in the literature,[33] and the slight difference between the two values is attributed to the C-H dipole decreasing the emission barrier of the CNTs.[34] The above comparison indicates that the accuracy of our calculations is good.
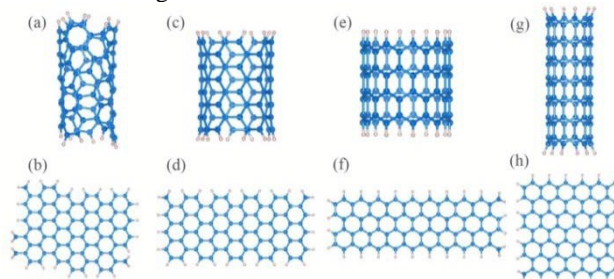
Fig. 2 Optimized ground-state structures of the neutral models in Fig. 1.
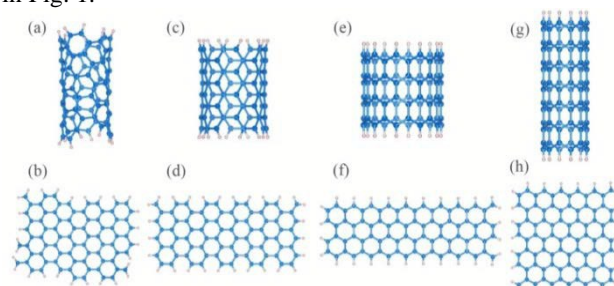
Fig. 3 Optimized ground-state structures of the models with one extra electron, which correspond to those in Fig. 2, respectively.

3 Results and discussion

3.1 HOMO energies of the (3,5) CNT and its corresponding GS containing 80 C atoms and carrying 0~8 extra electrons

Fig. 4(a) plots the HOMO energies of the (3,5) CNT and its GS counterpart, both of which contains 80 C atoms, against the amount of the extra electrons carried by them. The plots indicate that the HOMO energies of the two carbon nanomaterials both rise with the increase of the extra electron amount. When the amount is 0 or 1, their HOMO energies are negative, lower than the vacuum energy and close to each other. After the extra electron amount is increased to 2~8, the HOMO energies become positive and higher than the vacuum energy, implying that the electrons on the HOMO energies can easily escape into the vacuum and become secondary electrons when they are kicked by an external electron beam.[12,13,28,39] More significantly, in the cases with 2~8 extra electrons, the HOMO energy of the GS becomes remarkably lower than the one of the CNT, indicative of different rising modes. The rising rate of the former is 2.33 eV/electron, obviously lower than the one (2.66 eV/electron) of the latter. Further, the difference between the HOMO energies of the CNT and the GS is outlined in Fig. 4(b), manifesting that the difference generally increases with the increase of the extra electrons from 1 to 8 and reaches as high as 2.64 eV at the extra electrons of 8.

The above results mean that the rise of the HOMO energy of the CNT induced by negative charging is much greater and faster than that of the GS, and so the charged CNT can emit secondary electron more easily than the charged GS, conforming to our experimental results.[12,13] That is to say, the origin and mechanism of our experimental finding that the

secondary electron emission yields of CNTs are larger than that of graphene[12,13] is that the rise of the HOMO energy of a CNT induced by negative charging is much greater and faster than that of its corresponding GS with the same C atom amount. Although to inject extra 8 electrons to CNT and graphene in practice is very difficult, the above series of calculations give a solid trend shown in Fig. 4(b), indicating explicitly that our calculation finding can work after the amount of the extra electrons is larger than zero. Thus, the calculation finding would be performed in practice by charging CNT and graphene with nonzero extra electrons, which has been realized by our

experimental works.[12,13] Additionally, it should be noted that the (3, 5) CNT and GS models in Fig. 1(a, b) have 16 and 28 hydrogen atoms, respectively, along their edges. That is to say, the GS model has more hydrogen atoms than the CNT. To evaluate the effect of the extra hydrogen atoms on the HOMO change, we have calculated the HOMO energies of the GS models with 16 and 22 hydrogen atoms and found that the effect of the extra hydrogen atoms is negligible and the finding that the rise of the HOMO energy of the CNT induced by negative charging is much greater and faster than that of the GS still holds (see details in Supplementary Figs S1 and S2).
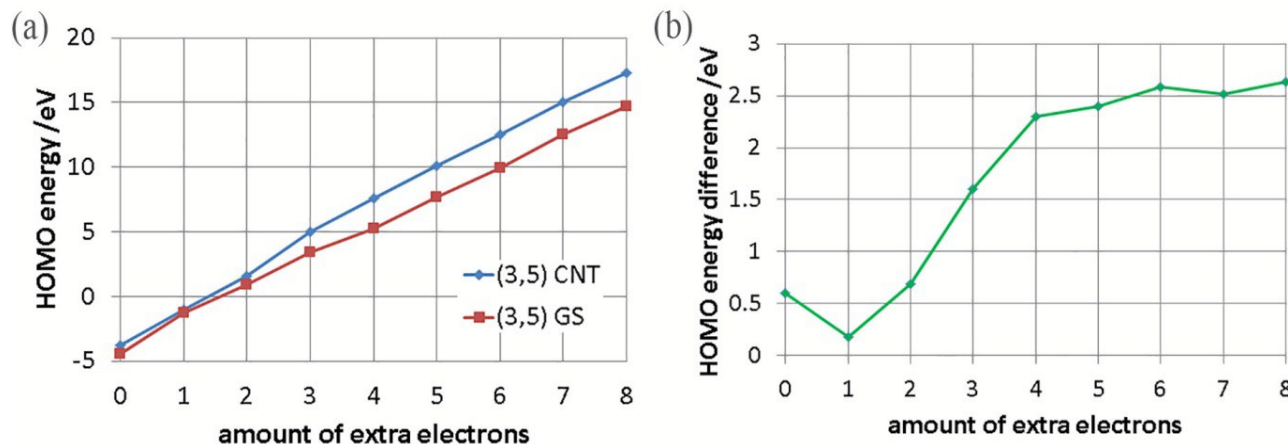
Fig. 4 (a) Dependences of the HOMO energies of the (3,5) CNT and its GS counterpart with 80 C atoms on the amount of the extra electrons, where the vacuum energy is set at 0 eV. (b) Dependence of the difference between the HOMO energies of the CNT and GS on the amount of the extra electrons, where the difference values were obtained by subtracting the HOMO energy of the GS from the one of the CNT.

In order to explore the reason why the rise of the HOMO energy of the (3,5) CNT induced by negative charging is much greater and faster than that of the GS, we have drawn the spatial distributions of the HOMOs of the models from the calculation results, as illustrated in Figs 5 and 6. The distributions show that in each of the cases charged with 0~8 extra electrons, the HOMO in the CNT is more closely packed than in the GS due to the geometry, leading to a larger Coulomb repulsion and thus a higher HOMO energy.
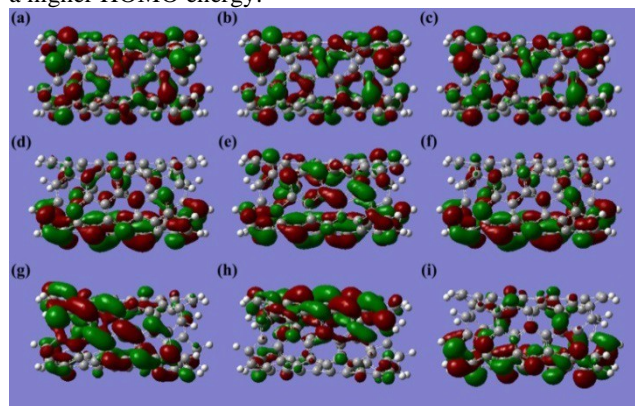
Fig. 5 Spatial distributions of the HOMOs of the (3,5) CNT containing 80 C atoms and charged by 0 (a), 1 (b), 2 (c), 3 (d), 4 (e), 5 (f), 6 (g), 7 (h) and 8 (i) extra electrons. The red and the green clouds denote the two different phases of the wave functions of the HOMOs. The asymmetry of the distributions is due to that the (3,5) CNT model is asymmetric.
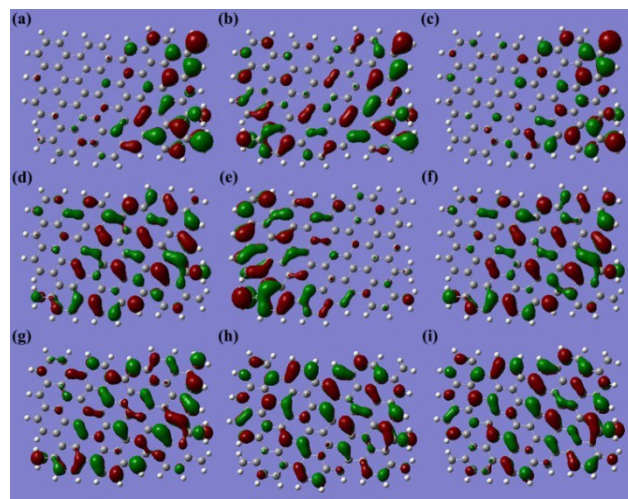
Fig. 6 Spatial distributions of the HOMOs of the GS counterpart of the (3,5) CNT containing 80 C atoms and charged by 0 (a), 1 (b), 2 (c), 3 (d), 4 (e), 5 (f), 6 (g), 7 (h) and 8 (i) extra electrons. The red and the green clouds denote the two different phases of the wave functions of the HOMOs. The asymmetry of the distributions is due to that the GS model was obtained by unzipping the CNT model and so is also asymmetric.

3.2 HOMO energies of the (3,5) CNTs and its corresponding GSs containing different amounts of C atoms and carrying 0~8 extra electrons

The results in Section 3.1 are only from the (3,5) CNT and GS containing 80 C atoms. Further, we calculated the (3,5) CNTs and GSs containing 60, 70, 90 and 100 C atoms, whose results are displayed in Fig. 7.
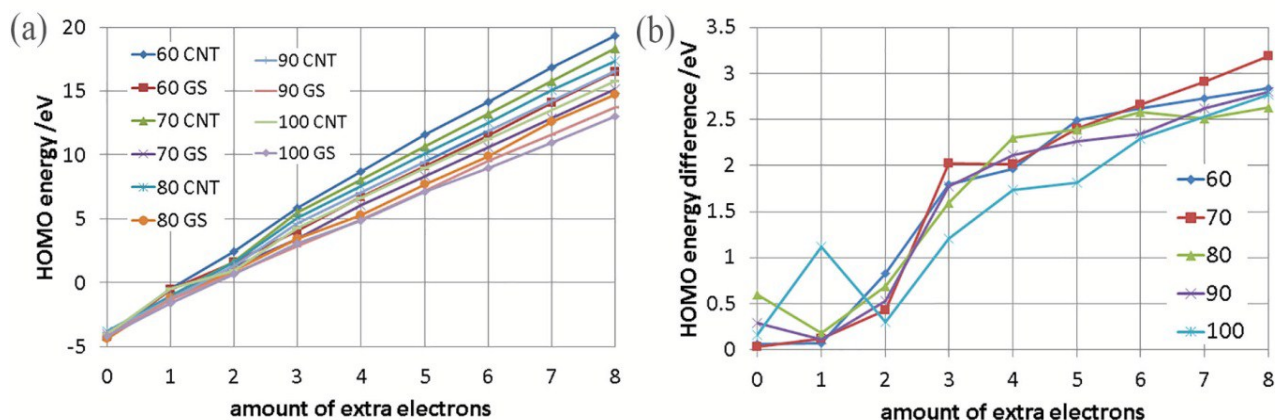
Fig. 7 (a) Dependences of the HOMO energies of the (3,5) CNTs and its GS counterparts on the amount of the extra electrons, where the amounts of the C atoms are labelled. (b) Dependence of the differences between the HOMO energies of the CNTs and GSs on the amount of the extra electrons.

Fig. 7 indicates that in all of the cases with 60, 70, 90 and 100 C atoms, the HOMO energies of the CNTs and GSs rise with the increase of the extra electron amount and become positive and higher than the vacuum energy after the extra electron amount is increased to 2~8. The rising rates of the HOMO energies of the CNTs are 2.92, 2.80, 2.57 and 2.44 eV/electron for 60, 70, 90 and 100 C atoms, respectively, all of which are obviously higher than those (2.53, 2.47, 2.21 and 2.11 eV/electron) of their GS counterparts. These comparison results are the same as those of the 80-C-atom case. The changing modes of the differences between the HOMO energies of the CNTs and GSs of 60, 70, 90 and 100 C atoms are also the same as that of the 80-C-atom case, except that the HOMO difference of 100 C atoms at the extra electron of 1 is

remarkably larger than the one at the extra electrons of 2. This exception does not overturn the theoretical finding that the rise of the HOMO energy of a CNT induced by negative charging is much greater and faster than that of its corresponding GS with the same C atom amount, because the HOMO energy of the CNT of 100 C atoms at the extra electron of 1 is still much higher than that of its GS counterpart and their HOMO difference generally increases with the increase of the extra electrons from 2 to 8. Moreover, the HOMO differences in the cases of 60, 70, 90 and 100 C atoms reach 2.84, 3.19, 2.80 and 2.77 eV at the extra electrons of 8, respectively, all of which are considerably large. The calculated values are listed in Table 1, for the sake of clear comparison.

Table 1 HOMO energy rising rates, HOMO energies and differences of the (3,5) CNTs and their corresponding GSs.

C atom amount	Model	HOMO energy rising rate (eV/electron)	HOMO energy (eV) at 8 extra electrons	CNT-GS HOMO energy difference (eV) at 8 extra electrons
60	CNT	2.92	19.32	2.84
	GS	2.53	16.48	
70	CNT	2.80	18.31	3.19
	GS	2.47	15.12	
80	CNT	2.66	17.33	2.64
	GS	2.33	14.69	
90	CNT	2.57	16.53	2.80
	GS	2.21	13.73	
100	CNT	2.44	15.77	2.77
	GS	2.11	13.00	

The above results indicate that the theoretical finding that the rise of the HOMO energy of a CNT induced by negative charging is much greater and faster than that of its corresponding GS with the same C atom amount holds regardless of the C atom amounts and so can be considered to be valid for infinite (3,5) CNT and graphene.

3.3 HOMO energies of the (5,5), (10,0) and (6,0) CNTs and their corresponding GSs carrying 0~8 extra electrons

The results in Sections 3.1 and 3.2 are only from the chiral (3,5) CNTs and their GS counterparts with different C atom amounts.

In order to check the universality of the theoretical finding that the rise of the HOMO energy of a CNT induced by negative charging is much greater and faster than that of graphene with the same C atom amount, we also calculated the (5,5), (10,0) and (6,0) CNTs and their GS counterparts containing 60, nearly 80 and nearly 100 C atoms. The (5,5), (10,0) and (6,0) CNTs are typically metallic armchair, semiconducting zigzag and metallic zigzag, respectively.[25,29]

Fig. 8 plots the HOMO energies and differences of the (5,5), (10,0), (6,0) CNTs and their corresponding GS counterparts, all of which contain nearly 100 C atoms, against the amount of the

extra electrons carried by them. Those of the CNTs and GSs with 60 and nearly 80 C atoms are given in Table 2.
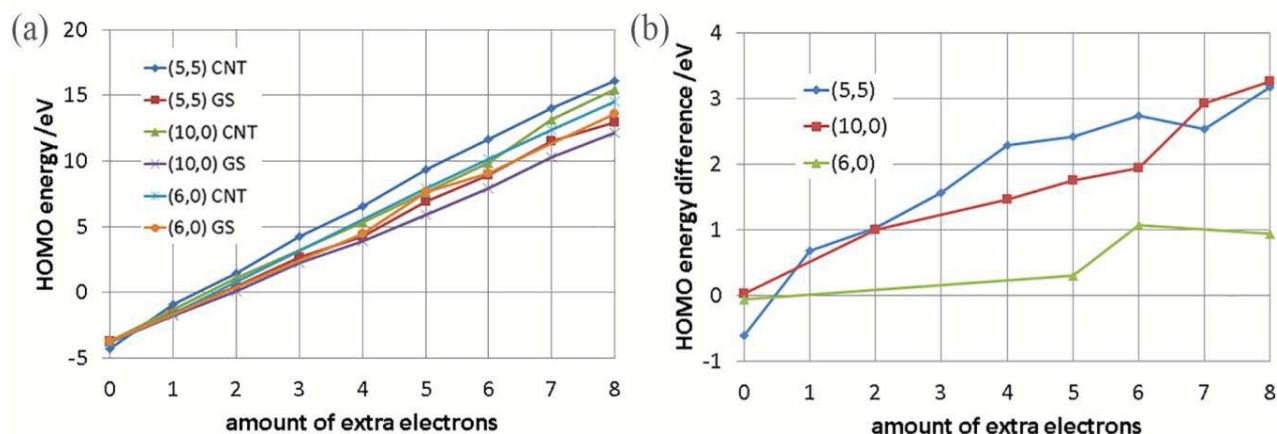
Fig. 8 (a) Dependences of the HOMO energies of the (5,5), (10,0) and (6,0) CNTs and their GS counterparts on the amount of the extra electrons, where the (5,5) and (10,0) CNTs and GSs contain 100 C atoms and the (6,0) ones contain 96. (b) Dependences of the differences between the HOMO energies of the CNTs and GSs on the amount of the extra electrons.

Table 2 HOMO energy rising rates, HOMO energies and differences of the (5,5), (10,0) and (6,0) CNTs and their GS counterparts. No data can be achieved for the blanks marked with the dash (-), due to non-convergence during the calculations. In the cases with ~ 80 C atoms, the C atom amounts of the (6,0) CNT and its GS are 84, and those of the other models are 80, where the slight difference is due to keep the edges of the (6,0) models as smooth as the others. In the cases with ~ 100 C atoms, the C atom amounts of the (6,0) models are 96, and those of the others are 100.

C atom amount	Model	HOMO energy rising rate (eV/electron)	HOMO energy (eV) at 8 extra electrons	CNT-GS HOMO energy difference (eV) at 8 extra electrons
60	(5,5) CNT	3.04	-	-
	GS	2.52	16.09	
	(10,0) CNT	2.78	18.46	2.98
	GS	2.34	15.48	
	(6,0) CNT	2.84	18.72	1.55
	GS	2.64	17.17	
~80	(5,5) CNT	2.72	17.55	3.00
	GS	2.33	14.55	
	(10,0) CNT	2.56	16.74	3.34
	GS	2.13	13.40	
	(6,0) CNT	2.56	14.63	-
	GS	2.33	-	
~100	(5,5) CNT	2.53	16.07	3.17
	GS	2.11	12.90	
	(10,0) CNT	2.38	15.43	3.25
	GS	1.99	12.18	
	(6,0) CNT	2.32	14.55	0.95
	GS	2.17	13.60	

We can see that the changing modes of the HOMO energies and differences of the (5,5), (10,0), (6,0) CNTs and their corresponding GS counterparts are the same as those of the (3,5) CNTs and GSs. All of their HOMO energies rise with the increase of the extra electron amount and become higher than the vacuum energy after the extra electron amount is increased to 2~8. The rising rates and the differences of their HOMO energies displayed in Table 2 indicate that the HOMO rising rates of the CNTs are all obviously larger than those of their GS counterparts and the HOMO differences of the CNTs and GSs generally increase with the increase of the extra electron amount from 1 to 8. These results indicate that the theoretical finding that the rise of the HOMO energy of a CNT induced by negative charging is much greater and faster than that of

graphene with the same C atom amount holds regardless of the CNT types.

4 Conclusions

Our first-principles calculations manifest quantitatively that the rise of the HOMO energy of a CNT induced by negative charging is much greater and faster than that of graphene with the same C atom amount. This finding holds regardless of the C atom amounts and the CNT types. This work reveals the origin and mechanism of the experimental results that the secondary electron emission yield of CNTs are much larger than those of graphene, and paves a new way to design and construct all-carbon devices with CNTs and graphene as different functional elements.

Acknowledgements

Notes and references

[a] National Center for Electron Microscopy in Beijing, School of Materials Science and Engineering, The State Key Laboratory of New Ceramics and Fine Processing, Key Laboratory of Advanced Materials (MOE), Tsinghua University, Beijing, 100084, P. R. China. Tel: +86 10 62782347, +86 10 62794026. E-mail address: jluo@mail.tsinghua.edu.cn (Jun Luo), jzhu@mail.tsinghua.edu.cn (Jing Zhu)

[b] Beijing Computational Science Research Center, Beijing 100084, P. R. China

[c] Beijing Institute of Nanoenergy and Nanosystems, Chinese Academy of Sciences, Beijing, 100083, P. R. China

[d] Center for Nano and Micro Mechanics, Tsinghua University, Beijing, 100084, P. R. China

[e] Department of Engineering Mechanics, School of Aerospace, Tsinghua University, Beijing, 100084, P. R. China

1   J. H. Warner, E. R. Margine, M. Mukai, A. W. Robertson, F. Giustino and A. I. Kirkland, *Science* , 2012, **337**, 209-212.

2   M. H. Rümmeli, C. G. Rocha, F. Ortmann, I. Ibrahim, H. Sevincli, F. Börrnert, J. Kunstmann, A. Bachmatiuk, M. Pötschke, M. Shiraishi, M. Meyyappan, B. Büchner, S. Roche and G. Cuniberti, *Adv. Mater.*, 2011, **23**, 4471-4490.

3   W. Zhou, M. D. Kapetanakis, M. P. Prange, S. T. Pantelides, S. J. Pennycook and J.C. Idrobo, *Phys. Rev. Lett.*, 2012, **109**, 206803.

4   X. M. Sun, S. Zaric, D. Daranciang, K. Welsher, Y. R. Lu, X. L. Li and H. J. Dai, *J. Am. Chem. Soc.*, 2008, **130**, 6551-6555.

5   W. Zhou, J. Lee, J. Nanda, S. T. Pantelides, S. J. Pennycook and J. C. Idrobo, *Nat. Nanotechnol.*, 2012, **7**, 161-165.

6   X. J. Zheng, J. Deng, N. Wang, D. H. Deng, W. H. Zhang, X. H. Bao and C. Li, *Angew. Chem. Int. Edit*, 2014, **53**, 7023-7027.

7   Z. Y. Zhang, F. Xiao, L. H. Qian, J. W. Xiao, S. Wang and Y. Q. Liu, *Adv. Energy. Mater.*, 2014, **4**, 1400064.

8   J. Luo, W. G. Ouyang, X. P. Li, Z. Jin, L. J. Yang, C. Q. Chen, J. Zhang, Y. Li, J. H. Warner, L. M. Peng L, Q. S. Zheng and J. Zhu, *Nano Lett.*, 2012, **12**, 3663-3667.

9   J. Zhao, M. R. He, S. Dai, J. Q. Huang, F. Wei and J. Zhu, *Carbon*, 2011, **49**, 206-213.

10 Z. S. Wu, S. F. Pei, W. C. Ren, D. M. Tang, L. B. Gao, B. L. Liu, F. Li, C. Liu and H. M. Cheng, *Adv. Mater.* 2009, **21**, 1756-1760.

11 C. Li, M. T. Cole, W. Lei, K. Qu, K. Ying, Y. Zhang, A. R. Robertson, J. H. Warner, S. Y. Ding, X. B. Zhang, B. P. Wang and W. I. Milne, *Adv. Funct. Mater.*, 2014, **24**, 1218-1227.

12 J. Luo, J. H. Warner, C. Q. Feng, Y. G. Yao, Z. Jin, H. L. Wang, C. F. Pan, S. Wang, L. J. Yang, Y. Li, J. Zhang, A. A. R. Watt, L. M. Peng, J. Zhu, and G. A. D. Briggs, *Appl. Phys. Lett*., 2010, **96**, 213113.

13 J. Luo, P. Tian, C. T. Pan, A. W. Robertson, J. H. Warner, E. W. Hill and G. A. D. Briggs, *ACS Nano*, 2011, **5**, 1047-1055.

14 R. Xu, Y. Sun, J. Y. Yang, L. He, C. J. Nie, L. L. Li and Y. D. Li, *Appl. Phys. Lett.*, 2010, **97**, 113101.

15 J. Li, X. B. Yan, G. Y. Gou, Z. Wang and J. T. Chen, *Phys. Chem. Chem. Phys.*, 2014, **16**, 1850-1855.

16 H. Y. Hao, P. Liu, J. Tang, Q. Cai and S. S. Fan, *Carbon*, 2012, **50**, 4203-4208.

17 J. Zhao, Q. Deng, A. Bachmatiuk, G. Sandeep, A. Popov, J. Eckert and M. H. Rümmeli, *Science*, 2014, **343**, 1228-1232.

18 F. Yang, X. Wang, D. Q. Zhang, J. Yang, D. Luo, Z. W. Xu, J. K. Wei, J. Q. Wang, Z. Xu, F. Peng, X. M. Li, R. M. Li, Y. L. Li, M. H. Li, X. D. Bai, F. Ding and Y. Li, *Nature*, 2014, **510**, 522-524.

19 Y. B. Chen, Y. Y. Zhang, Y. Hu, L. X. Kang, S. C. Zhang, H. H. Xie, D. Liu, Q. C. Zhao, Q. W. Li and J. Zhang, *Adv. Mater.*, 2014, **26**, 5898-5922.

20 X. L. Wei, S. Wang, Q. Chen and L. M. Peng, *Sci. Rep.*, 2014, **4**, 5102.

21 A. W. Robertson, G. D. Lee, K. He, E. Yoon, A. I. Kirkland and J. H. Warner, *Nano Lett.*, 2014, **14**, 1634-1642.

22 B. I. Yakobson and F. Ding, *ACS Nano*, 2011, **5**, 1569-1574.

23 J. Zhao, M. Shaygan, J. Eckert, M. Meyyappan and M. H. Rümmeli, *Nano Lett.*, 2014, **14**, 3064-3071.

24 J. H. Warner, G. D. Lee, K. He, A. W. Robertson, E. Yoon and A. I. Kirkland, ACS Nano, 2013, **7**, 9860-9866.

25 B. Shan and K. Cho, *Phys. Rev. Lett.*, 2005, **94**, 236602.

26 R. Ruoff, *Nat. Nanotechnol.*, 2008, **3**, 10-11.

27 E. S. Penev, V. I. Artyukhov, F. Ding and B. I. Yakobson, *Adv. Mater.*, 2012, **24**, 4956-4976.

28 A. Nojeh, B. Shan, K. Cho and R. F. W. Pease, *Phys. Rev. Lett.*, 2006, **96**, 056802.

29 J. Luo, L. M. Peng, Z. Q. Xue and J. L. Wu, *Phys. Rev. B,* 2002, **66**, 115415.

30 J. Y. Lu, S. P. Gao and J. Yuan, *Ultramicroscopy*, 2012, **112**, 61-68.

31 J. T. Lü, T. Gunst, P. Hedegård and M. Brandbyge, *Beilstein J. Nanotechnol.*, 2011, **2**, 814-823.

32 T. Gunst, J. T. Lü, P. Hedegård and M. Brandbyge, *Phys. Rev. B*, 2013, **88**, 161401.

33 J. J. Zhao, J. Han and J. P. Lu, *Phys. Rev. B*, 2002, **65**, 193401.

34 G. H. Chen, Z. B. Li, J. Peng, C. S. He, W. L. Wang, S. Z. Deng, N. S. Xu, Y. C. Wang, S. Y. Wang, X. Zheng, G. H. Chen and T. Yu, *J. Phys. Chem. C*, 2007, **111**, 4939-4945.

35 C. Yu, H. M. Liu, W. B. Ni, N. Y. Gao, J. W. Zhao and H. L. Zhang, *Phys. Chem. Chem. Phys.*, 2011, **13**, 3461-3467.

36 L. C. Xu, R. Z. Wang, M. S. Miao, X. L. Wei, Y. P. Chen, H. Yan, W. M. Lau, L. M. Liu and Y. M. Ma, *Nanoscale*, 2014, **6**, 1113.

37 X. Jiang, J. J. Zhao, Y. L. Li and R. Ahuja, *Adv. Funct. Mater.*, 2013, **23**, 5846-5853.

38 Q. G. Jiang, Z. M. Ao and Q. Jiang, *Phys. Chem. Chem. Phys.*, 2013, **15**, 10859-10865.

39 G. T. Mearini, I. L. Krainsky, J. J. A. Dayton, Y. Wang, C. A. Zorman, J. C. Angus and R. W. Hoffman, *Appl. Phys. Lett.*, 1994, **65**, 2702-2704.

40 A. D. Becke. *J. Chem. Phys.*, 1993, **98**, 5648-5652.

41 C. Lee, W. Yang and R. G. Parr, *Phys. Rev. B*, 1988, **37**, 785.

42 R. Krishnan, J. S. Binkley, R. Seeger and J. A. Pople, *J. Chem. Phys.*, 1980, **72**, 650-654.

43 M. K. Shukla, M. Dubey and J. Leszczynski, *ACS Nano*, 2008, **2**, 227-234.

44 M. J. Frisch, G. W. Trucks, H. B. Schlegel, G. E. Scuseria, M. A. Robb, J. R. Cheeseman, G. Scalmani, V. Barone, B. Mennucci, G. A. Petersson, H. Nakatsuji, M. Caricato, X. Li, H. P. Hratchian, A. F. Izmaylov, J. Bloino, G. Zheng, J. L. Sonnenberg, M. Hada, M. Ehara, K. Toyota, R. Fukuda, J. Hasegawa, M. Ishida, T. Nakajima, Y. Honda, O. Kitao, H. Nakai, T. Vreven, J. A. Montgomery, J. E. Peralta, F. Ogliaro, M. Bearpark, J. J. Heyd, E. Brothers, K. N. Kudin, V. N. Staroverov, R. Kobayashi, J. Normand, K. Raghavachari, A. Rendell, J. C. Burant, S. S. Iyengar, J. Tomasi, M. Cossi, N. Rega, J. M. Millam, M. Klene, J. E. Knox, J. B. Cross, V. Bakken, C. Adamo, J. Jaramillo, R. Gomperts, R. E. Stratmann, O. Yazyev, A. J. Austin, R. Cammi, C. Pomelli, J. W. Ochterski, R. L. Martin, K. Morokuma, V. G. Zakrzewski, G. A. Voth, P. Salvador, J. J. Dannenberg, S. Dapprich, A. D. Daniels, O. Farkas, J. B. Foresman, J. V. Ortiz, J. Cioslowski and D. J. Fox, *Gaussian 09, Revision **B.01***, 2009.